BMC Pulmonary Medicine

RESEARCH

Open Access

TRIM11 Prevents Ferroptosis in model of asthma by UBE2N-TAX1BP1 signaling

Na Li[1*], Guoqing Qiu[1], Xiangqin Xu[1], Yan Shen[1] and Yuming Chen[1]

Abstract

Asthma is a complex chronic respiratory inflammatory disease affected by both genetic and environmental factors. Therefore, our study explored the influence of TRIM11 on asthma and its underlying mechanisms. Our research involved patients diagnosed with asthma and healthy volunteers recruited from our hospital. We observed a reduction in serum TRIM11 expression in asthma patients, which positively correlated with the levels of anti-IgE or IgE. Additionally, both TRIM11 mRNA and protein expression in lung tissue were diminished. The introduction of the TRIM11 gene resulted in a reduction in inflammation in an in vitro asthma model and prevented the development of asthma in a mouse model. Moreover, the TRIM11 gene exhibited a suppressive effect on Ferroptosis and mitigated ROS-induced mitochondrial damage in the asthma model. TRIM11 was found to stimulate UBE2N-TAX1BP1 signaling in the asthma model, with UBE2N being identified as the specific target for TRIM11's effects on Ferroptosis. Furthermore, TRIM11 protein interacted with UBE2N protein and facilitated the dissociation of UBE2N-UBE2N in the asthma model. In conclusion, TRIM11 plays a vital role in preventing Ferroptosis in the asthma model through UBE2N-TAX1BP1 signaling. This indicates that targeting the TRIM11 mechanism could serve as a promising strategy for anti-Ferroptosis immunotherapy in asthma treatment.

Keywords TRIM11, Ferroptosis, Asthma, TAX1BP1

Introduction

Asthma, a complex chronic respiratory inflammatory disorder, is influenced by a combination of genetic and environmental factors [1]. Common manifestations encompass wheezing, chest tightness, and persistent coughing [1]. Children constitute a demographic group with a high prevalence of asthma, yet the precise pathologic mechanism remains enigmatic. Notably, a pattern of familial aggregation is accompanied by numerous triggering factors and individual variabilities [2]. Allergens such as air pollution, secondhand smoke, airborne catkins, pollen, and other stimulants are hypothesized to contribute to asthma exacerbations. Moreover, respiratory infections and psychological stress, including anger, have been identified as potential triggers for asthma attacks. Improving asthma control in pediatric patients diagnosed with asthma has emerged as a crucial focus within the medical community [3, 4].

Ferroptosis, a newly discovered form of cell death, showcases distinct morphological and biochemical characteristics [5, 6]. Central to the pathologic mechanism of asthma is the damage and death of airway epithelial cells. Thus, safeguarding these cells to sustain airway epithelial integrity emerges as a promising therapeutic avenue for asthma management [5, 6]. Epidemiological data reveals a progressive increase in the incidence of childhood asthma yearly [5, 6]. Currently, hormone-based control constitutes as the primary treatment strategy for

*Correspondence:
Na Li
Linda5204@163.com
[1]Department of Respiratory and Critical Care Medicine, Longgang Central Hospital, 6082 Longgang Avenue, Shenzhen 518116, China

asthma; nevertheless, the effectiveness of hormones in severe asthma cases remains less than ideal. Increasingly, research indicates the significant role that Ferroptosis plays in the initiation and progression of asthma [5].

The protein TAX1BP1 assumes a critical role in influencing cell proliferation, activation, and apoptosis [7]. Research indicates that TAX1BP1 operates by suppressing the activation of ERK and the expression of Blimp-1, thereby governing the formation of B cell Germinal centers and modulating B cell activation and differentiation [8]. Furthermore, the combined action of TAX1BP1 and the ubiquitin editing enzyme A20 synergistically inhibits the NF-κB and IRF3 signaling pathways, consequently exhibiting anti-apoptotic effects [9].

UBE2N, a ubiquitin- conjugating enzyme, performs various functions and is involved in a variety of immune disorders and cancers [10]. Notably, the downregulation of UBE2N results in a substantial decrease in melanoma cell proliferation and subcutaneous tumor growth [11]. Furthermore, silencing UBE2N can alleviate apoptosis in laryngeal squamous cell carcinoma cells induced by radiation, thereby reinforcing the radiation resistance of these cells [12].

TRIM11 (tripartite motif-containing protein 11) functions as a ubiquitin E3 ligase [13]. Studies have shown that TRIM11 acts as an oncogene in various malignancies, demonstrating upregulation in liver cancer, colon cancer, human brain malignant glioma, and lung cancer. It promotes tumor cell proliferation, invasion, and migration [14–16]. Consequently, our research explores the impact of TRIM11 on asthma and elucidates its underlying mechanisms.

Materials and methods

Patients experiment

Patients with asthma and normal healthy volunteers were obtained from our hospital. This study was approved by the Ethics Committee of our hospital (no: 202106250912). Serum was collected and immediately stored at -80 °C (Table 1).

The diagnostic criteria for CVA refer to the Diagnosis and Treatment Guidelines for Cough (2015).

The selection criteria are (1) age range from 18 to 60 years old. (2) Meets the diagnostic criteria for asthma in the bronchial asthma prevention and treatment guidelines formulated by the Chinese Medical Association. (3) The first diagnosis was asthma, and there was no regular anti asthma treatment before. (4) The clinical data is complete, including general information, medical history, chest X-ray/CT, lung function, induced sputum cytology count, FeNO, VAS score, and cough symptom score.

The exclusion criteria are: (1) Chest imaging suggests the presence of other lung diseases. (2) Individuals who use angiotensin-converting enzyme inhibitor drugs and have severe dysfunction in important organs such as the heart, brain, liver, and kidney, as well as a history of malignant tumors. (3) Systemic glucocorticoid users.

Table 1 Basic information of patients included

Group	Normal	Patients
Number	12	12
Age	46.08 ± 17.49	47.75 ± 14.72
Sex	Male: 6, Female: 6.	Male: 6, Female: 6.

Quantitative PCR

The total RNA was extracted from all samples using a TRIZOL reagent (Life Technologies Inc.). qRT-PCR assays were performed using Light Cycler® 480 SYBR Mix (Roche, Germany). The expression levels of mRNA were normalized to the GAPDH expression using the $2^{-\Delta\Delta CT}$ method. Primers used for qRT-PCR: TRIM11: CAGGATGCGTTGCTGTTCCAAG and AAACGGCGAAGACGCTCGAACT; β-actin: GTCTCCTCTGACTTCAACAGCG and ACCACCCTGTTGCTGTAGCCAA.

Mice experiment

This animal experiment was approved by the Ethics Committee of our hospital (no: 20230122053). All mice were purchased from Animal Experiment Center of Shenzhen University and were randomly allocated into sham (number=6), asthma (number=6) group. Next, all mice were randomly allocated into vector (asthma+vector=6), sh-FUNDC1 (asthma+TRIM11=6, number=6) group. C57BL/6 mice (5–6 weeks, male, 17–19 g) in control group were challenged with intranasal instillation of 30 μl of saline for 12 days. Mice in model group were challenged with intranasal instillation of HDM (10 μg in 30 μl of saline) for 12 days, as previously described [17]. Mice in vector group were challenged with intranasal instillation of HDM (10 μg in 30 μl of saline), and injected with 1.5×10^9 plaque-forming units of recombinant vector virus (200 μL/mice) via the tail vein for 12 days. Mice in si-FUNDC1 group were challenged with intranasal instillation of HDM (10 μg in 30 μl of saline), and injected with 1.5×10^9 plaque-forming units of recombinant si-FUNDC1 virus (200 μL/mice) via the tail vein for 12 days.

Then, all mice were randomly allocated into vector (asthma+vector=6), si-FUNDC1 (asthma+sh-FUNDC1=6, number=6), si-FUNDC1+FBXL2 (asthma+sh-FUNDC1+FBXL2 agonists=6, number=6) group. The mice were injected with 1.5×10^9 plaque-forming units of recombinant vector virus or recombinant si- FUNDC1 virus or recombinant si-FUNDC1 virus+FBXL2 agonists (30 μg/kg of BC-1258, MedChemExpress, Shanghai, China) in 200 μL of phosphate-buffered saline (PBS) via the tail vein.

BALF was analyzed as previously described [17]. the BALF was absorbed by an 1mL syringe. Then repeat

the perfusion and aspiration 3 times without waiting for filling. The supernatants of the first BALF were used to measure cytokines. All BALF cells were collected for FACS analyses.

Histological examination and immunofluorescence

Lung tissue samples were fixed in 4% paraformaldehyde, paraffn-embedded and then sectioned into 5 μm slices for H&E staining. Lung injury scored and immunofluorescence according to the following criteria [18]: 1, normal; 2, minimal (little) damage; 3, mild damage; 4, moderate damage; 5, severe damage; and 6, maximal damage. Tissue was treated with primary antibodies anti-TRIM11 (ab111694, 1:100, abcam) for 12 h. Nuclei were stained with DAPI and cells were observed under a fluorescent illumination microscope (Olympus IX71, Tokyo, Japan).

Immunofluorescence and Western blot analysis

Cells were fixed with 4% paraformaldehyde, permeabilized with 0.5% Triton X-100 in PBS for 15 min at room temperature, and blocked with 5% BSA for 30 min at 37 °C. Cells were treated with primary antibodies at 4 °C overnight: anti- TRIM11 and anti- UBE2N. Cells were then incubated with Cy3-conjugated goat anti-rabbit or goat anti-mouse IgG DyLight 555-conjugated secondary antibodies for 2 h at 37 °C. Nuclei were stained with DAPI and cells were observed under a fluorescent illumination microscope (Olympus IX71, Tokyo, Japan).

Total protein was extracted from lung samples or cell samples using Radio-Immunoprecipitation Assay (RIPA) and PMSF reagent (1:100, Beyotime, Beijing, China). Protein lysates were separated based on their molecular weight on SDS/PAGE gels and transferred onto a Polyvinylidene Fluoride (PVDF) membrane. The membrane was blocked with non-fat-milk (5%) for 2 h at room temperature and incubated with anti-TRIM11(ab111694, 1:1000, abcam), anti- UBE2N (ab109286, 1:1000, abcam), anti- TAX1BP1 antibody (ab176572, 1:1000, abcam) and anti-β-actin antibody (1:10000, ab8226, abcam) at 4 °C overnight. Then first antibodies were removed and TBST wash membrane using TBST. Membranes were incubated with the secondary antibody for 2 h at room temperature. The bound antibodies were detected using enhanced chemiluminescence (ECL).

Cell culture and RNA transfection

A549 cell line were cultured in Dulbecco's modified eagle's medium (DMEM, Gibco) supplemented with 10% fetal bovine serum (FBS, Gibco) in an incubator at 37 °C with 5% CO2. A549 cell was transfected with Negative plasmid (Negative group), FUNDC1 plasmid (FUNDC1 group), si-nc plasmid (si-nc group), si-FUNDC1 plasmid (si-FUNDC1 group) using Lipofectamine 3000. After 48 h, A549 cell treated with 200 ng/ml of LPS (L5293, Sigma, Shanghai, China) for 4 h and then pulsed with ATP (1 mM, Sigma-Aldrich, MO, USA) for 30 min.

ELISA kits and electron microscopy

Tissue in each groupwere homogenized with PBS and PMSF reagent (1:100, Beyotime, Beijing, China), and were collected at 2000 g for 10 min at 4 °C. Cell samples were collected at 2000 g for 10 min at 4 °C. IgE (H493-1), HDM IgE (H107-1-1), iron kit (A039-1-1), IL-4 (H005-1-2), IL-5 (H006), IL-10 (H009-1-2) and IL-13 (H011) kits (Nanjing Jiancheng Biotechnology Research Institute) were used to measure the cytokine levels.

MTT assay kit (ST316), LDH release kit (C0016), calcein/PI kit (C2015S), GSH activity (S0053), JC-1 aggregation (C2003S), ROS production (S0033S) (Beyotime) were used to measure the cytokine levels.

Electron microscopy were executed according to the previously described using a Hitachi H7650 transmission electron microscope (Tokyo, Japan) at 80 Kv [17].

Bioluminescence imaging and 3D structures for protein structureA549-hUBE2N -Luc were structured according to the previously described [19]. Bioluminescent imaging was performed using an IVIS imaging system (Bio-Real, QuickView3000, Austria). This study used PDB (https://www1.rcsb.org/) and uniprot (https://www.uniprot.org/uniprotkb/).

Statistical analysis

Data were expressed as mean ± SD. Multiple comparisons were used GraphPad Prism 8 to perform by Student's t-test or one-way ANOVA followed by Tukey's post-test. P values < 0.05 were considered statistically significant.

Results

TRIM11 expression level in the asthma model

The study explores the potential significance of TRIM11 in asthma patients. Notably, a decrease in serum TRIM11 expression was observed in individuals with asthma (Fig. 1A). Furthermore, a negative correlation was observed between serum TRIM11 levels and anti-HDM IgE protein or IgE in asthma patients (Fig. 1B and C). AUC analysis was carried out to evaluate the diagnostic value of TRIM11 in asthma patients (Fig. 1D). In an asthma mouse model, both TRIM11 mRNA and protein expression in lung tissue demonstrated reductions (Fig. 1E and F). Immunofluorescence analysis revealed decreased TRIM11 expression in lung tissue of the asthma mouse model (Fig. 1G). Hence, TRIM11 appears to be downregulated during the progression of the disease related to it.

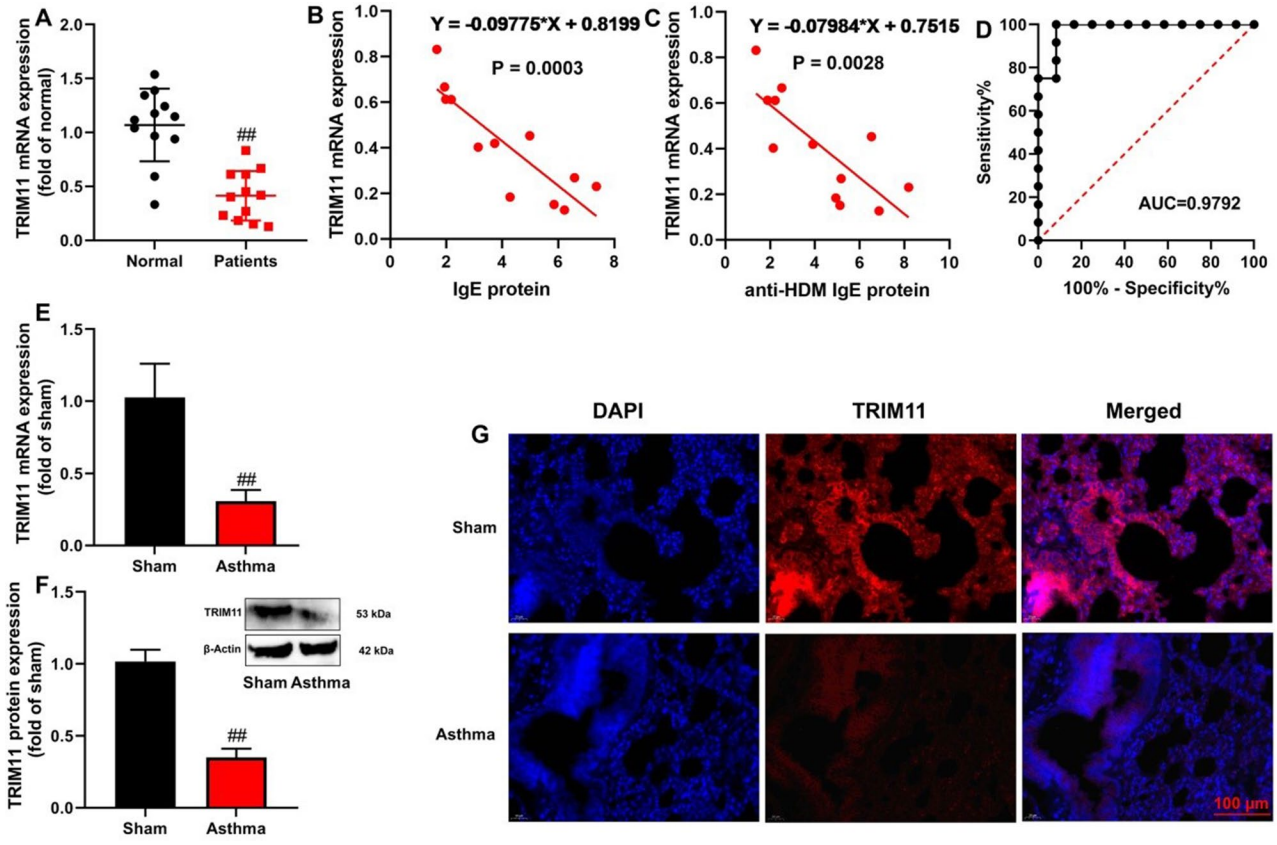

Fig. 1 TRIM11 expression level in model of asthma. TRIM11 expression (**A**), the expression of serum TRIM11 was positive correlation with anti-HDM IgE protein or IgE in patients with asthma (**B**, **C**), diagnostic value of TRIM11 (**D**) in patients with asthma; TRIM11 mRNA and protein expression (**E**, **F**), TRIM11 expression (Immunofluorescence, **G**) in mice model of asthma. $^{\#\#}p < 0.01$ compared with normal or sham group. Number of patients = 12, number of mice = 6

The TRIM11 gene alleviated inflammation in the in vitro model of asthma

Subsequently, we enhanced TRIM11 expression using a TRIM11 plasmid, which led to reduced TRIM11 expression in an in vitro asthma model through si-TRIM11 plasmid intervention (Fig. 2A). The upregulation of TRIM11 led to decreased activity levels of IL-4, IL-5, IL-10, and IL-13 in the in vitro asthma model (Fig. 2B). Conversely, downregulating TRIM11 expression increased the activity levels of IL-4, IL-5, IL-10, and IL-13 in the in vitro asthma model (Fig. 2C).

Si-TRIM11 gene facilitated the development of asthma in the mouse model

The research assessed the impact of TRIM11 on asthma using a mouse model. The si-TRIM11 virus significantly increased the HE score, thereby acting as a prophylactic measure for asthma (HE staining). Additionally, it led to enhanced levels of serum HDM-specific IgE, serum IgE, while expansion IL-4, IL-5, IL-10, and IL-13 activity levels in the lung tissue of the mouse model (Fig. 3). In conclusion, by regulating asthma-related factors, the si-TRIM11 gene effectively promoted the onset of asthma in the model.

The TRIM11 gene mitigated ferroptosis in model of asthma

The study investigated the function of TRIM11 in ferroptosis within an asthma model. Upregulation of the TRIM11 gene enhanced cell viability and GSH activity levels, while reducing LDH and PI positive cells, along with lowering iron content in an in vitro asthma model (Fig. 4A and E). Conversely, downregulation of the TRIM11 gene impaired cell viability and GSH activity, increased LDH and PI positive cells, and elevated iron content in the in vitro asthma model (Fig. 4F and J). Notably, TRIM11 gene suppression led to decreased GPX4 protein expression, whereas TRIM11 overexpression resulted in elevated GPX4 protein levels in the in vitro asthma model (Fig. 4K and L). Additionally, the administration of the TRIM11 virus augmented GSH activity and GPX4 protein expression in a mouse model of asthma (Fig. 4M and N).

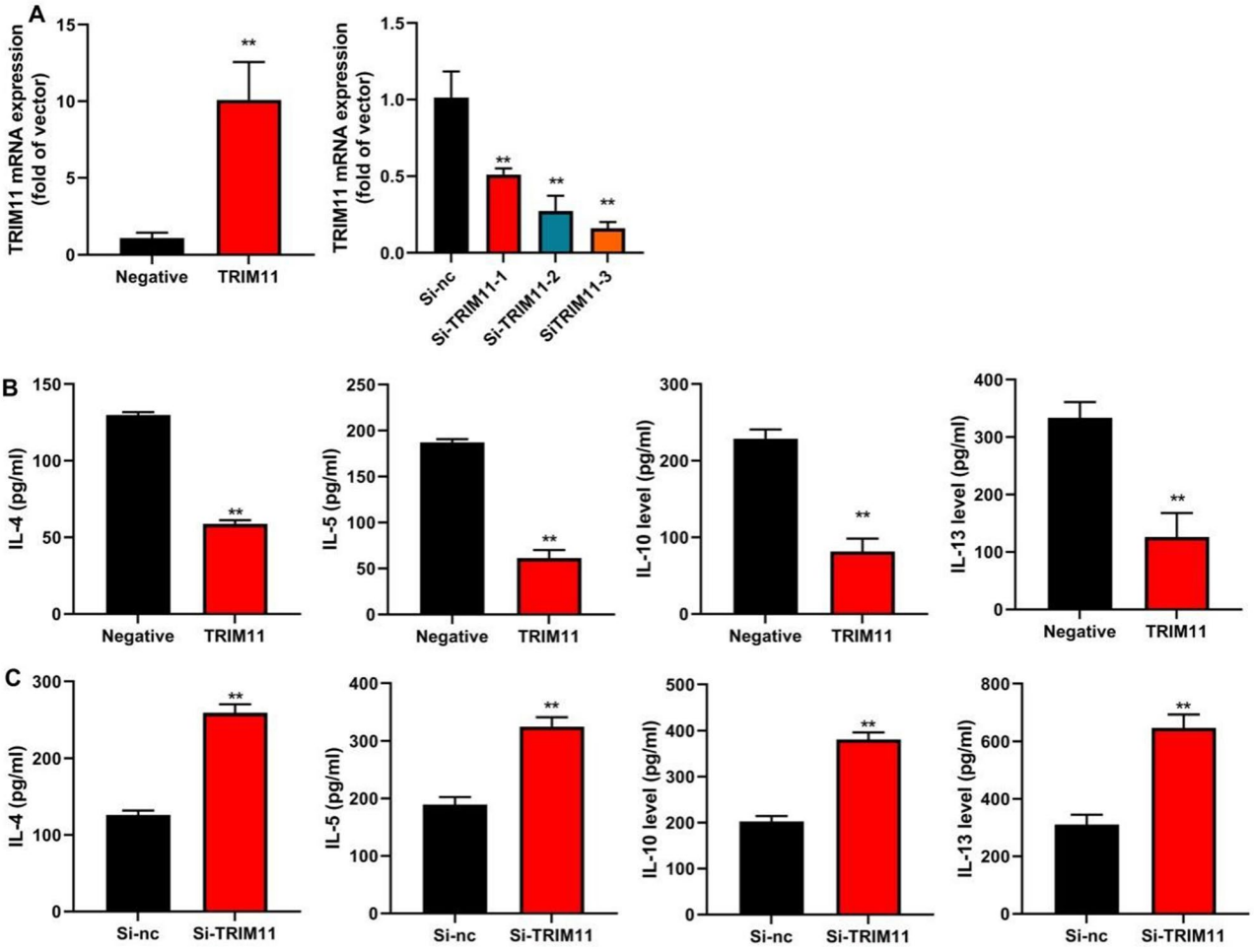

Fig. 2 TRIM11 gene reduced inflammation in vitro model of asthma. TRIM11 expression (**A**), IL-4, IL-5, IL-10 and IL-13 activity levels in vitro mode by TRIM11 plasmid (**B**); IL-4, IL-5, IL-10 and IL-13 activity levels in vitro mode by si-TRIM11 plasmid (**C**). $^{**}p < 0.01$ compared with negative or si-nc group. Number of vitro model = 3

The TRIM11 gene alleviated ROS-mitochondrial damage in model of asthma

The study probed into the mechanism of the TRIM11 gene in association with ferroptosis in a mouse model of asthma. Elevating TRIM11 gene expression led to increased JC-1 and calcein-AM/CoCl2 levels, while mitigating ROS-induced mitochondrial damage in an in vitro asthma model (Fig. 5A, C and G). In contrast, reducing TRIM11 gene expression resulted in diminished JC-1 and calcein-AM/CoCl2 levels, along with enhanced ROS-induced mitochondrial damage in the in vitro asthma model (Fig. 5D, F and H).

TRIM11 elicited UBE2N-TAX1BP1 signaling in model of asthma

The experiment probed into the mechanism behind TRIM11 in relation to ferroptosis and ROS-induced mitochondrial damage within an asthma model. Elevating TRIM11 gene expression triggered an increase in UBE2N mRNA levels, whereas reducing TRIM11 gene expression inhibited UBE2N mRNA levels in the in vitro asthma model (Fig. 6A). Moreover, the introduction of TRIM11 virus led to an augmentation of UBE2N protein expression and diminished TAX1BP1 protein expression in the lung tissue of mice in the asthma model (Fig. 6B). Simultaneously, upregulating the TRIM11 gene stimulated TRIM11 and UBE2N protein expressions, while suppressing TAX1BP1 protein expressions in the in vitro asthma model (Fig. 6C). Conversely, downregulating the TRIM11 gene decreased TRIM11 and UBE2N protein expressions, and promoted TAX1BP1 protein expressions in the in vitro asthma model (Fig. 6D).

UBE2N serves as the target spot for the effects of TRIM11 on ferroptosis in model of asthma

To explore the influence of TRIM11 on ferroptosis in this model, an inhibitor of UBE2N (Ubc13, NSC697923 from MedChemExpress) was utilized. Administration of the

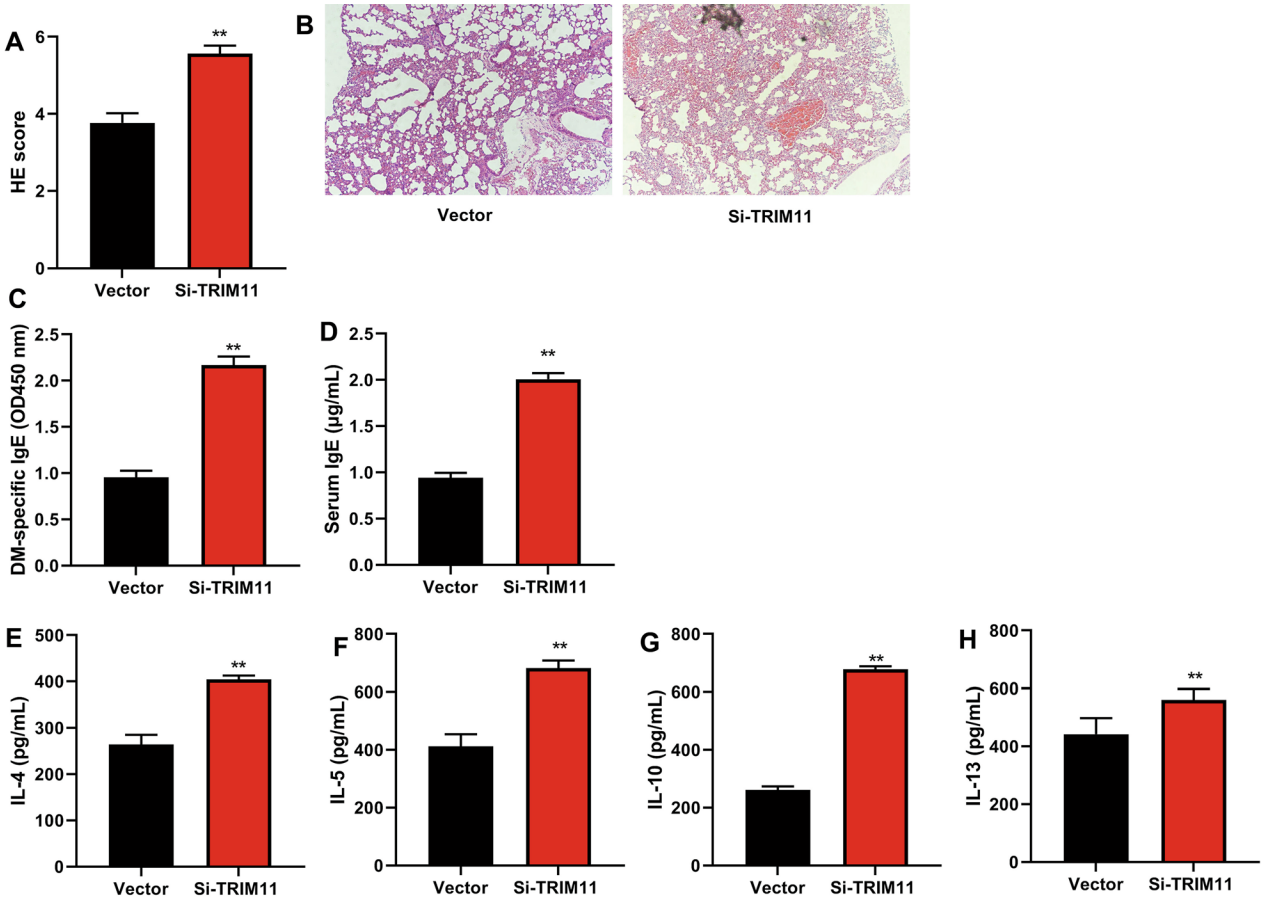

Fig. 3 Si-TRIM11 gene promoted asthma in mice model. HE score (**A**), HE staining (**B**), serum HDM-specific IgE (**C**), serum IgE (**D**), IL-4/IL-5/IL-10/IL-13 activity levels (**E**, **F**, **G**, **H**) in mice model. $^{**}p < 0.01$ compared with vector group. Number of mice = 6

UBE2N inhibitor (5 mg/kg) resulted in the downregulation of UBE2N and GPX4 protein expressions, along with an upregulation of TAX1BP1 protein expression in the lung tissue of mice with asthma (Fig. 7A). The UBE2N inhibitor not only exacerbated asthma symptoms, HE scores, and IL-4/IL-5/IL-10/IL-13 activity levels in the lung tissue of mice exposed to the TRIM11 virus (Fig. 7B -K). Subsequently, in the in vitro asthma model, the UBE2N inhibitor (2 μM) also suppressed UBE2N and GPX4 protein expressions, while inducing TAX1BP1 protein expression (Figure S1A).

Furthermore, the UBE2N inhibitor augmented IL-4/IL-5/IL-10/IL-13 activity levels, decreased cell viability, elevated LDH, calcein-AM/CoCl2 levels, and iron content, as well as reduced JC-1 and calcein-AM/CoCl2 levels in the in vitro asthma model (Figure S1B, S2). In conclusion, the UBE2N protein serves as a target for the effects of TRIM11 on ferroptosis in an asthma model.

TRIM11 protein is interlinked with UBE2N protein

The study investigated the regulatory mechanism of TRIM11 on UBE2N in an asthma model. By employing a 3D model prediction, it was discovered that the TRIM11 protein interacted with the UBE2N protein. Specifically, residues PRO-457, ARG-286, ARG-341, and GLU-411 of TRIM11 formed hydrogen bonds with ASN-31, TYR-34, MET-72, and LYS-74 of UBE2N, respectively. The lengths of these hydrogen bonds were measured to 3.1Å, 2.8Å, 2.7Å, and 3.3Å, respectively, suggesting potential roles of these residues in the activities of both proteins (Fig. 8A).

Subsequently, a mutation was introduced as depicted in Fig. 8B. Immunoprecipitation (IP) analysis demonstrated that TRIM11 WT protein interacted with UBE2N WT protein, while TRIM11 WT protein did not interact with UBE2N Mut protein, and TRIM11 Mut protein did not link with UBE2N WT protein (Fig. 8C). Immunofluorescence imaging displayed that upregulation of TRIM11 increased both TRIM11 and UBE2N expression in the in vitro asthma model (Fig. 8D). Additionally, upregulation of led to decreased UBE2N ubiquitin levels, whereas downregulation of TRIM11 resulted in increased UBE2N ubiquitin in the in vitro asthma model (Fig. 8E).

Furthermore, bioluminescence imaging disclosed that sh-TRIM11 reduced UBE2N expression in the lung tissue

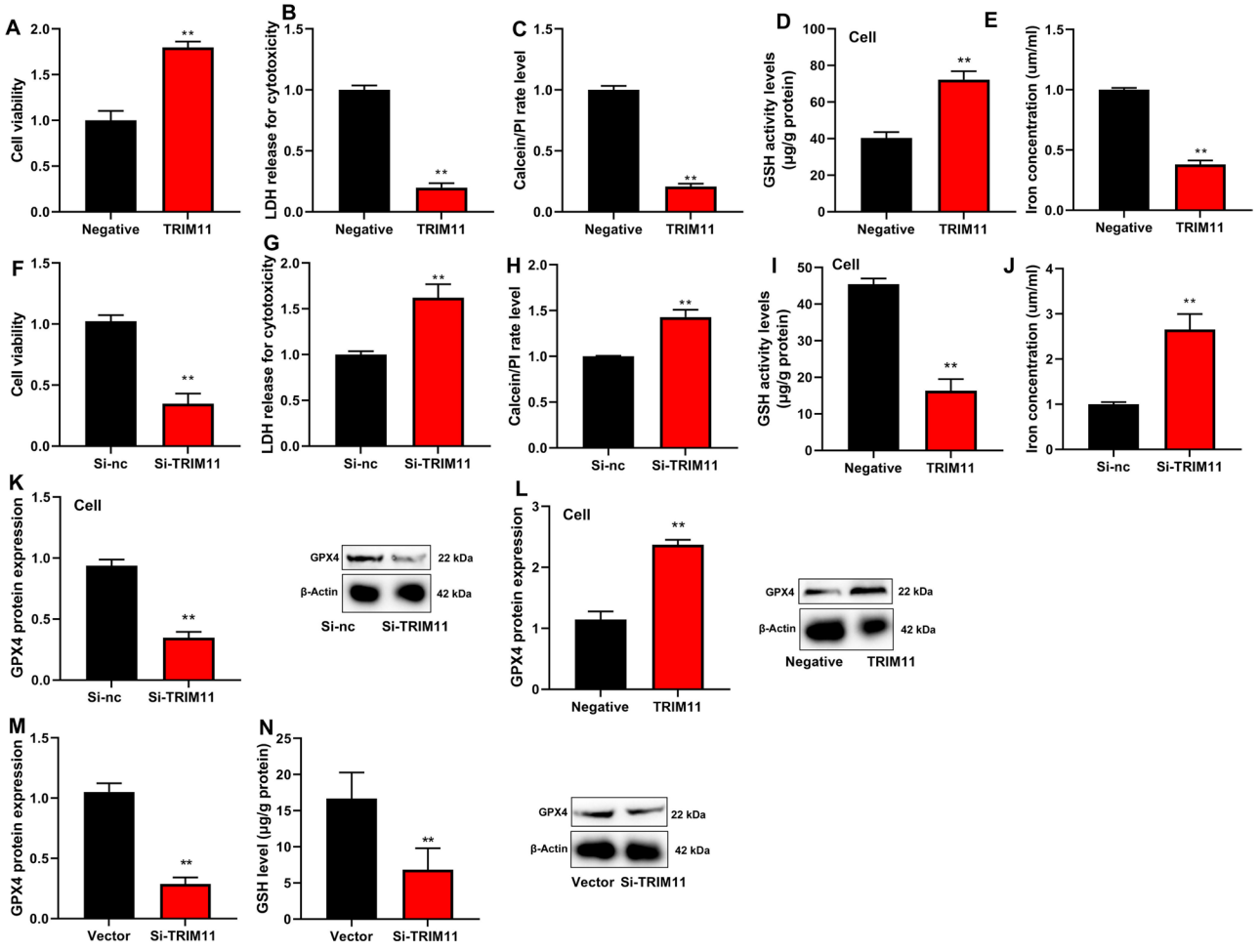

Fig. 4 TRIM11 gene reduced Ferroptosis in model of asthma. Cell viability (**A**), LDH and PI positive cells (**B**, **C**), GSH activity level (**D**), iron content (**E**) in vitro mode by TRIM11 plasmid; cell viability (**F**), LDH and PI positive cells (**G**, **H**), GSH activity level (**I**), iron content (**J**) in vitro mode by si-TRIM11 plasmid; GPX4 protein expression (**K**, **L**), GSH activity and GPX4 protein expression (**M**, **N**). $^{**}p < 0.01$ compared with negative or si-nc or vector group. Number of vitro model = 3, number of mice = 6

of the mouse model (Fig. 8F). These discoveries imply that TRIM11 protein interacts with UBE2N protein to reduce UBE2N ubiquitin levels in the asthma model.

TRIM11 facilitated the dissociation of UBE2N-TAX1BP1 in model of asthma

The study investigated the regulatory mechanism of TRIM11 on UBE2N in an asthma model. Through the utilization of a 3D model prediction, it was revealed that the TRIM11 protein interacted with the UBE2N protein, whereby residues PRO-457, ARG-286, ARG-341, and GLU-411 of TRIM11 formed hydrogen bonds with ASN-31, TYR-34, MET-72, and LYS-74 of UBE2N, respectively. The lengths of these hydrogen bonds were measured to be 3.1Å, 2.8Å, 2.7Å, and 3.3Å, respectively, indicating potential roles of these residues in the activities of both proteins (Fig. 9A). Subsequently, a mutation was introduced as depicted in Fig. 9B. Immunoprecipitation (IP) analysis manifested that TRIM11 WT protein interacted with UBE2N WT protein, while TRIM11 WT protein did not interact with UBE2N Mut protein, and TRIM11 Mut protein did not link with UBE2N WT protein (Fig. 9C). Immunofluorescence imaging exhibited that upregulation of TRIM11 increased both TRIM11 and UBE2N expression in the in vitro asthma model (Fig. 9D). Additionally, TRIM11 upregulation led to attenuated UBE2N ubiquitin levels, whereas TRIM11 downregulation induced an increased UBE2N ubiquitin in the in vitro asthma model (Fig. 9E). Furthermore, bioluminescence imaging disclosed that sh-TRIM11 reduced UBE2N expression in the lung tissue of the mouse model (Fig. 9F). These revelations imply that TRIM11 protein interacts with UBE2N protein to reduce UBE2N ubiquitin levels in the asthma model.

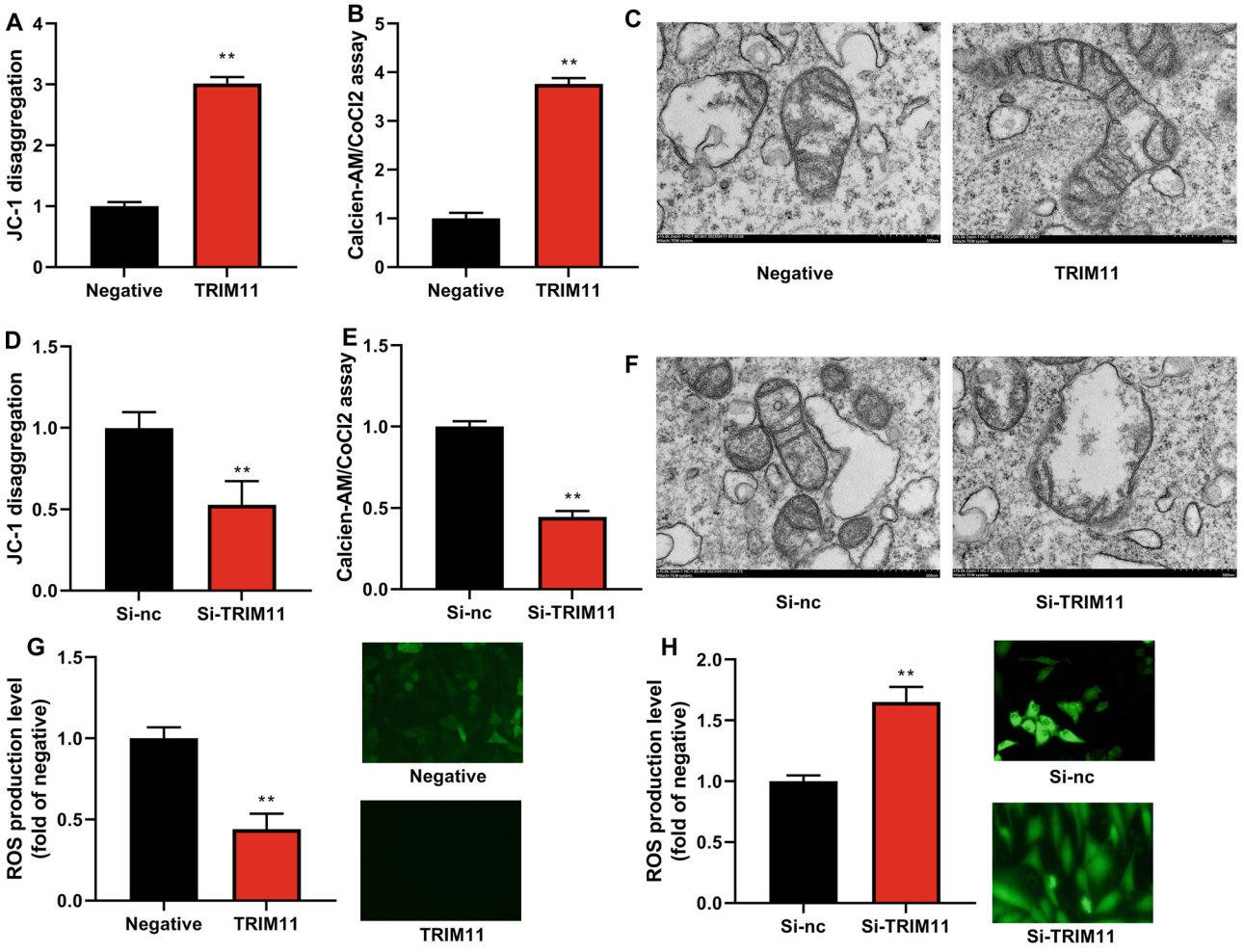

Fig. 5 TRIM11 gene reduced ROS-mitochondrial damage in model of asthma. JC-1 (**A**), calcien-AM/CoCl2 levels (**B**), mitochondrial damage (**C**) in vitro mode by TRIM11 plasmid; JC-1 (**D**), calcien-AM/CoCl2 levels (**E**), mitochondrial damage (**F**) in vitro mode by si-TRIM11 plasmid; ROS levels (**G** and **H**). $^{**}p < 0.01$ compared with negative or si-nc group. Number of vitro model = 3

Discussion

Bronchial asthma, often referred to as asthma, is a chronic inflammatory disorder of the respiratory system associated with airway hyperresponsiveness involving Eosinophils, Mast cells, and other related cellular components [20]. Primarily affecting children, asthma is characterized by widespread and variable reversible airflow obstruction [20]. The precise etiology remains incompletely understood. Recurrent symptoms such as wheezing, chest tightness, and cough necessitate long-term standardized and personalized treatment to minimize symptom frequency and severity as much as possible [21]. However, the clinical efficacy of symptom control in many pediatric asthma cases is currently suboptimal, possibly due to various triggers. Reports suggest that asthma attacks can be triggered by factors such as smoking, air pollution, respiratory infections, inhalation of distilled water droplets or cold air, and psychological influences. Therefore, in addition to standardized therapy, strengthening environmental control is equally crucial [21]. In this investigation, the expression of serum TRIM11 was found to be downregulated in asthma patients or mouse models. The TRIM11 gene exhibited a protective role against asthma and reduced inflammation in both in vitro asthma models and mouse models. Liu et al. have identified that TRIM11 diminishes inflammasome activity in human inflammatory disorders [22]. These findings suggest that TRIM11 plays a beneficial role in asthma by supporting protective effects through FUNDC1.

Ferroptosis assumes a pivotal role in the pathogenesis and progression of asthma, along with its contribution in regulating tumors, ischemia-reperfusion injury, acute kidney injury, and other conditions [23]. The cytopathological traits observed in lung tissue of asthmatic mice closely resemble the cellular morphology associated with Ferroptosis: reduction of Crista, rupturing and shrinking of the outer membrane. These resemblances

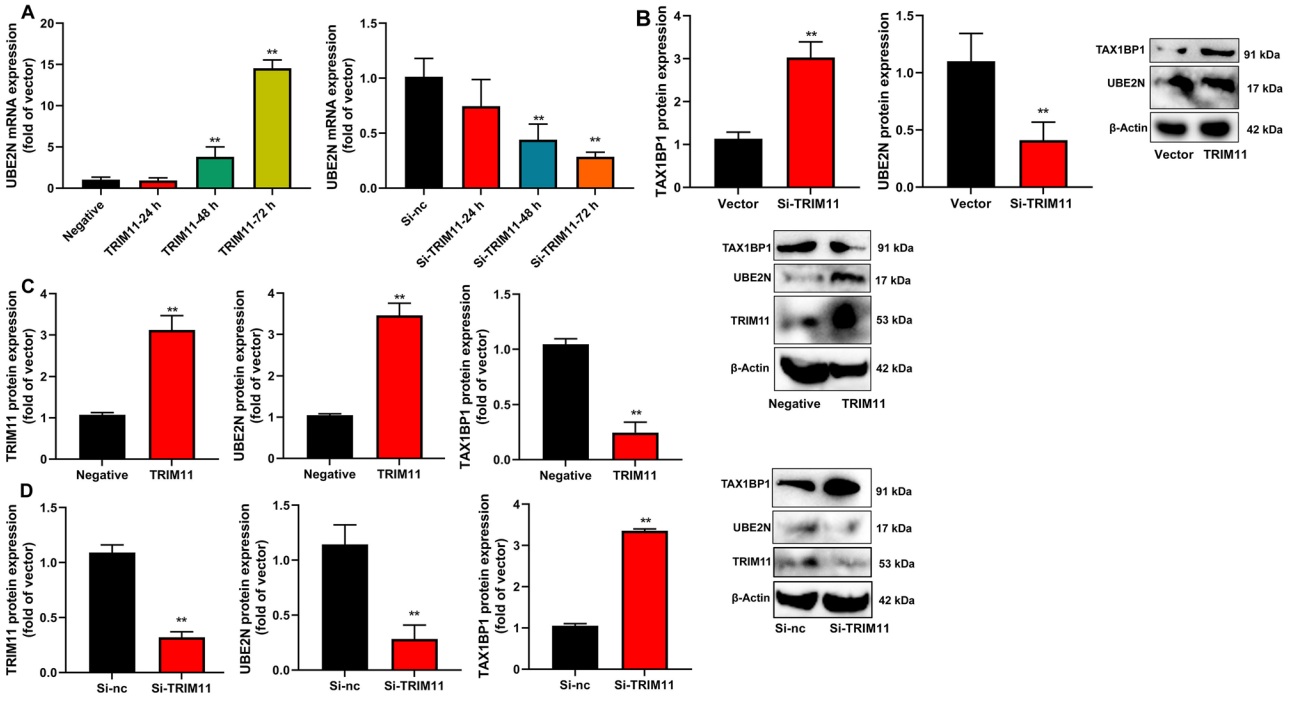

Fig. 6 TRIM11 induced UBE2N-TAX1BP1 signaling in model of asthma. UBE2N mRNA expression (**A**), RIM11 and UBE2N protein expressions (**B**), TRIM11/UBE2N/TAX1BP protein (**C** and **D**)., $^{**}p < 0.01$ compared with negative or si-nc group. Number of vitro model = 3, number of mice = 3

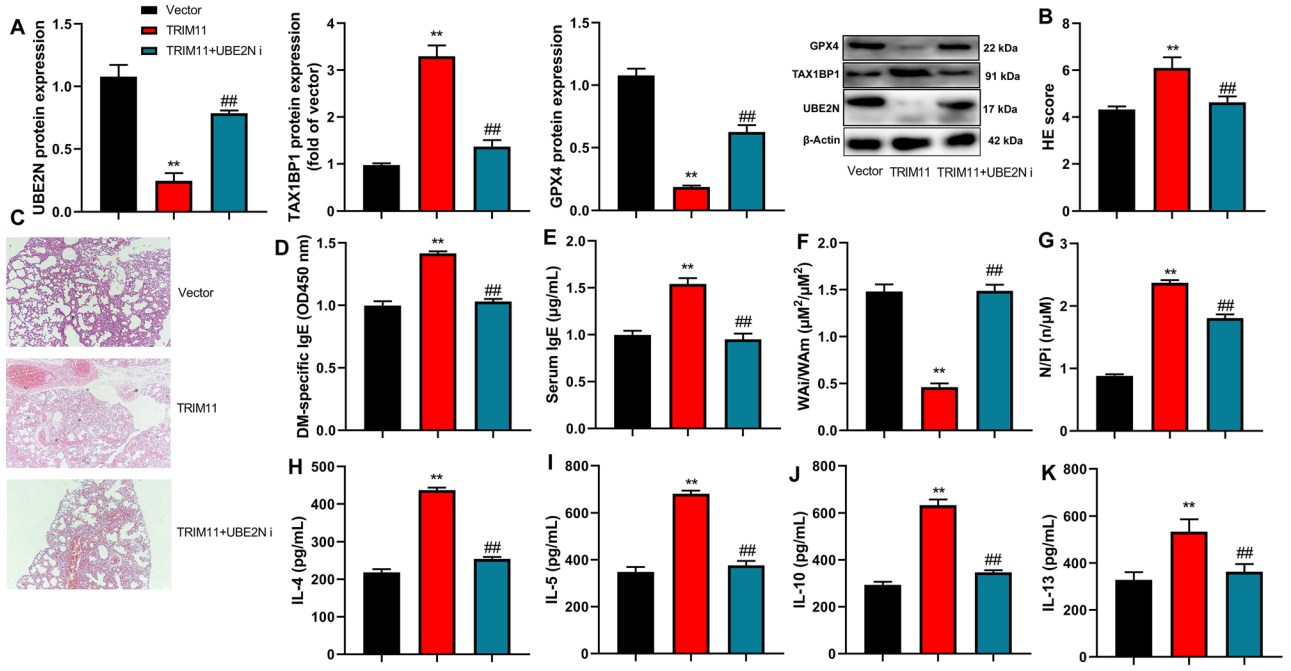

Fig. 7 UBE2N is target spot for the effects of TRIM11 on Ferroptosis in model of asthma. TRIM11/UBE2N/TAX1BP protein (**A**), HE score (**B**), HE staining (**C**), serum HDM-specific IgE (**D**), serum IgE (**E**), N/Pi (**F**), Wai/WAm (**G**), IL-4/IL-5/IL-10/IL-13 activity levels (**H**–**K**) in mice model. $^{**}p < 0.01$ compared with vector group, $^{\#\#}p < 0.01$ compared with TRIM11 group. Number of vitro model = 3, number of mice = 6

indicate a potentially intimate relationship between asthma and Ferroptosis [24]. Current research on the interaction between Ferroptosis and asthma primarily focuses on airway epithelial cell Ferroptosis [25]. Our discoveries suggest that the TRIM11 gene alleviates Ferroptosis and ROS-induced mitochondrial damage in the asthma model. Shang et al. have demonstrated that TRIM11 suppresses ferritinophagy in pancreatic ductal

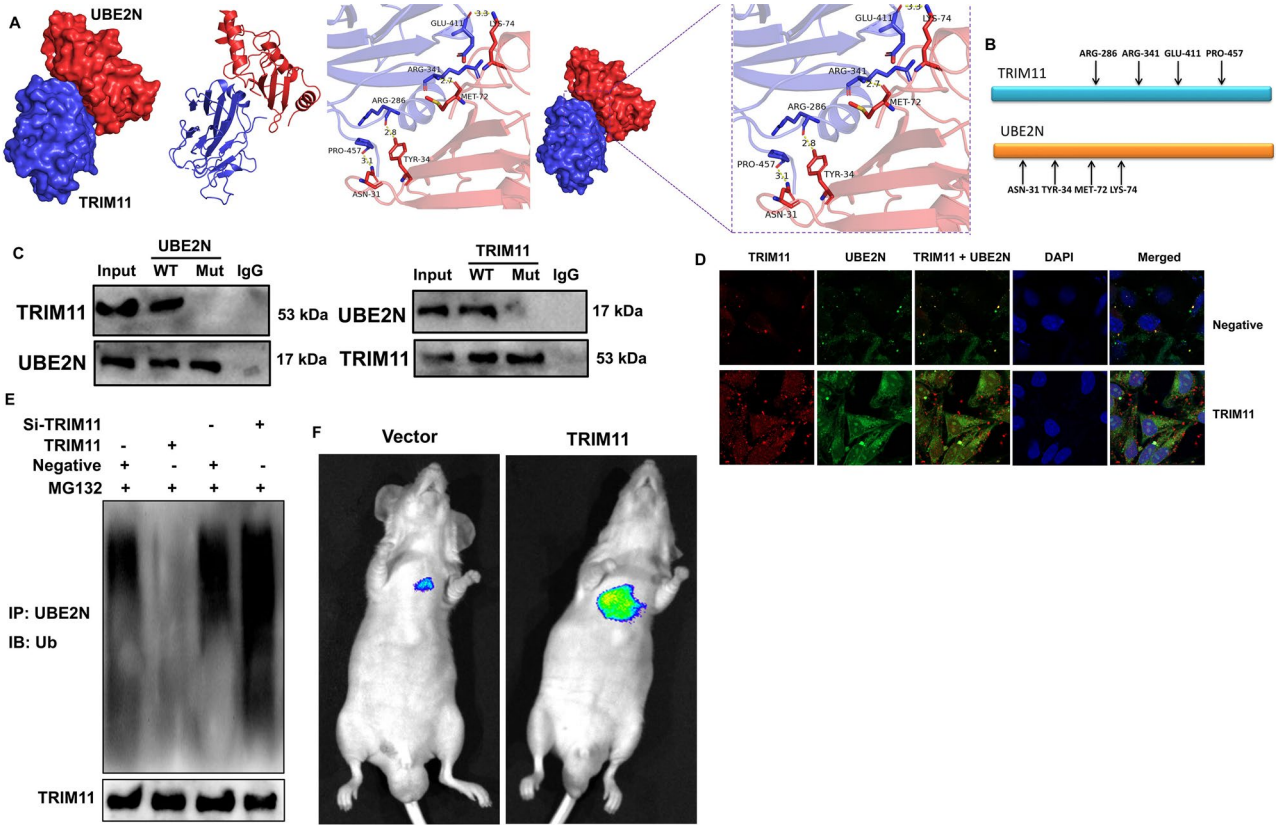

Fig. 8 TRIM11 protein interlinked with UBE2N protein. 3D structure for TRIM11 protein interlinking with UBE2N protein (**A**), Mutation site of TRIM11 or UBE2N (**B**), IP assay for TRIM11 protein interlinking with UBE2N protein (**C**), immunofluorescence for TRIM11 protein interlinking with UBE2N protein (**D**); UBE2N Ubiquitination (**E**), UBE2N expression in lung tissue of mice model (**F**). Number of vitro model = 3, number of mice = 3

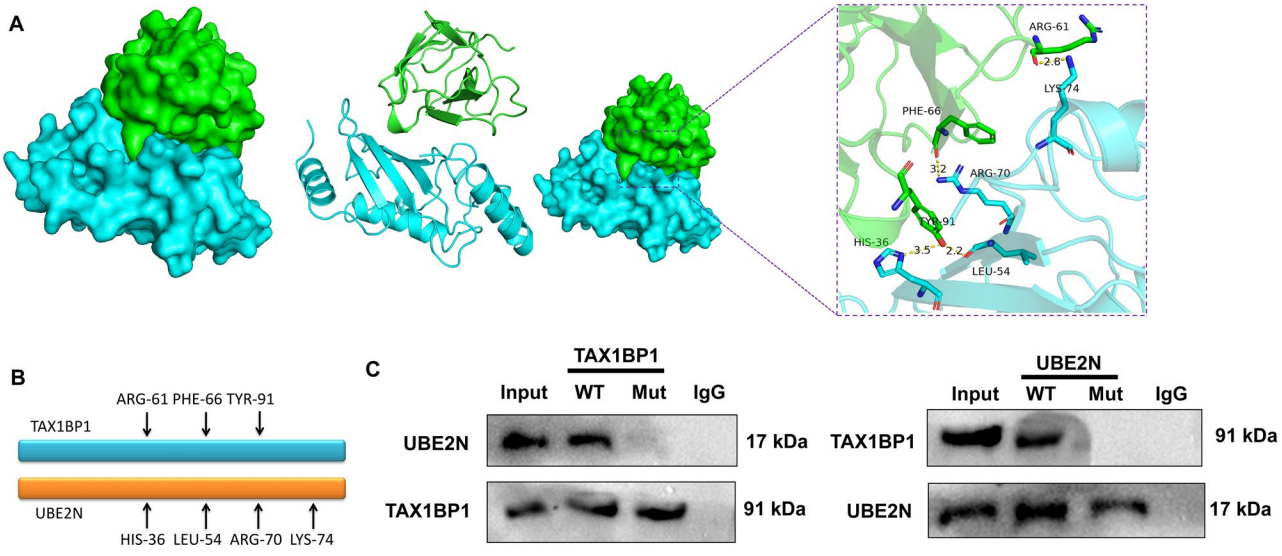

Fig. 9 UBE2N protein interlinked with TAX1BP1 protein. 3D structure for TAX1BP1 protein interlinking with UBE2N protein (**A**), IP assay for TAX1BP1 protein interlinking with UBE2N protein (**B**), immunofluorescence for TRIM11 protein interlinking with UBE2N protein (**C**). Number of vitro model = 3

adenocarcinoma [26]. These results strongly imply that TRIM11 acts against Ferroptosis in asthma through ROS-induced mitochondrial damage. Given that asthma often occurs in childhood, our experiment using mice of 5–6 weeks as a model has a little difference from the clinical practice. This constitutes the deficiency of this study. We aim to study the mice for 1–2 weeks in the subsequent step, which is better approximated to the clinical reality.

TAX1BP1 participates in non-lipid-dependent autophagy and operates independently of the autophagy protein ATG7, depending instead on the SKICH domain and a newly identified N-domain of TAX1BP1 [27]. The SKICH domain disrupts the association between TBK1 and FIP200, facilitating FIP200 aggregation around NBR1 and promoting continual Autophagosome formation [28]. Therefore, to characterize the B cell autophagy modulated by TAX1BP1, it is crucial to assess LC3 lipid-related proteins [9]. This research disclosed that TRIM11 triggers UBE2N-TAX1BP1 signaling in the asthma model. UBE2N acts as the target for TRIM11's impact on Ferroptosis in the asthma model. Shang et al. have demonstrated that TRIM11 inhibits ferritinophagy in pancreatic ductal adenocarcinoma via UBE2N/TAX1BP1 signaling [26]. These findings illustrate that TRIM11 induces UBE2N-TAX1BP1 signaling to counteract ferroptosis in the context of asthma.

In Parkin-mediated mitochondrial autophagy, UBE2N, UBE2L3, and UBE2D2/3 collaboratively contribute to the process. Additionally, UBE2N and UBE2D3 are crucial for the aggregation of mitochondrial proteins in antiviral innate immunity [29]. UBE2N plays a significant regulatory role in the proliferation of cancer cells [30]. Within this study, it was observed that TRIM11 protein interacts with the UBE2N protein, facilitating the dissociation of UBE2N-TAX1BP1 in the asthma model. Shembade et al. have proposed that UBE2N regulates TAX1BP1 signaling [31]. These results demonstrate that TRIM11 induces UBE2N-TAX1BP1 signaling to safeguard against ferroptosis in asthma by alleviating ROS-induced mitochondrial damage. In conclusion, TRIM11 prevents Ferroptosis in asthma model by UBE2N-TAX1BP1 signaling via ROS-mitochondrial damage (Fig. 10). This indicates that targeting this TRIM11-mediated mechanism may potentially serve as a feasible strategy for anti-ferroptosis immunotherapy in asthma.

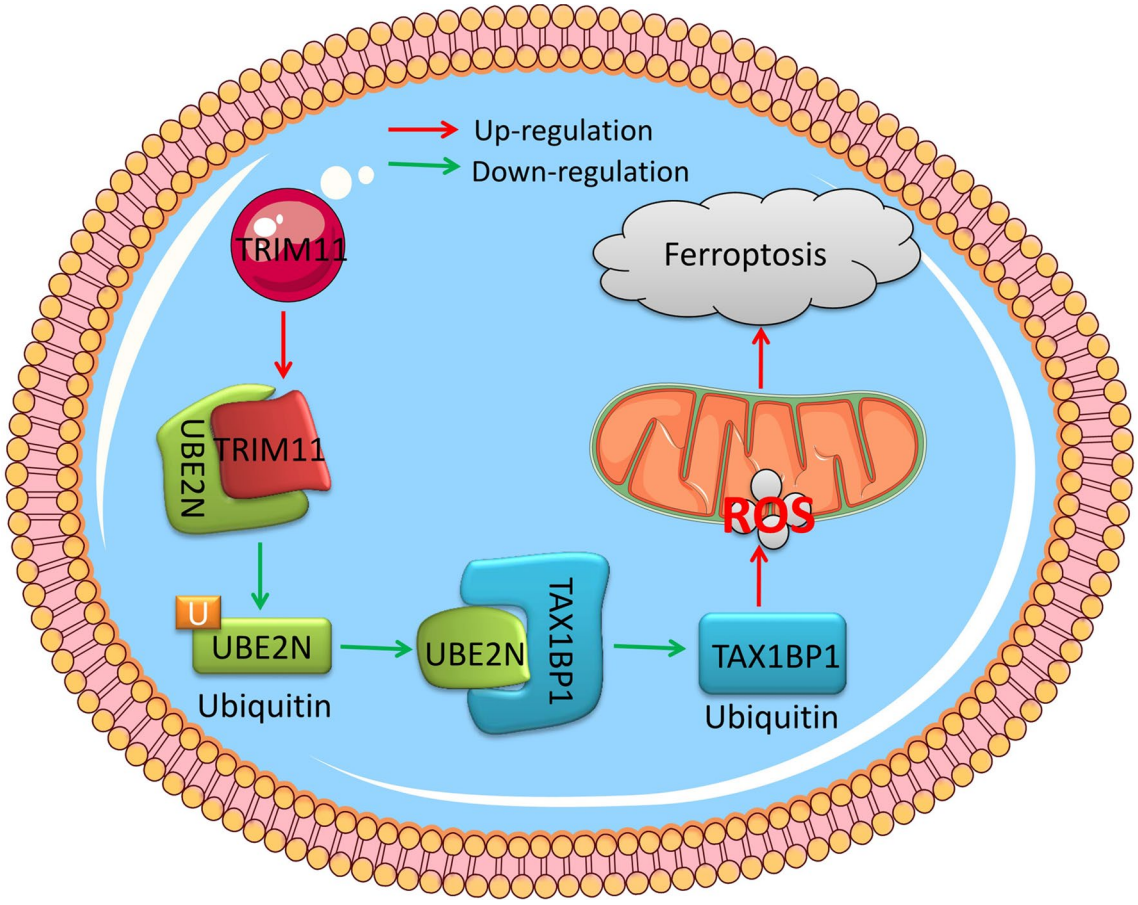

Fig. 10 TRIM11 Prevents Ferroptosis in model of asthma by UBE2N-TAX1BP1 signaling

Supplementary Information

The online version contains supplementary material available at https://doi.org/10.1186/s12890-024-03351-9.

Supplementary Material 1: Figure S1. TRIM11 gene reduced inflammation in vitro model of asthma. TRIM11/UBE2N/ TAX1BP protein (A), IL-4/IL-5/ IL-10/IL-13 activity levels (B). **p<0.01 compared with negative group, ##p<0.01 compared with TRIM11 group. Number of vitro model = 3, number of mice = 6.

Supplementary Material 2: Figure S2. TRIM11 gene reduced Ferroptosis in model of asthma. Cell viability (A), LDH and PI positive cells (B, C), iron content (D), calcien-AM/CoCl2 levels (E), JC-1 (F). **p<0.01 compared with negative group, ##p<0.01 compared with TRIM11 group. Number of vitro model = 3.

Supplementary Material 3

Supplementary Material 4

Acknowledgements
Not applicable.

Author contributions
NL designed the experiments. GQQ and XQX performed the experiments. YS and YMC collected and analyzed the data. NL, YS and YMC drafted manuscript. All authors read and approved the final manuscript.

Funding
Not applicable.

Data availability
The datasets used and/or analyzed during the current study available from the corresponding author on reasonable request.

Declarations

Ethics approval and consent to participate
The current study was approved by the Ethics Committee of Longgang Central Hospital(no: 20230122053)(no: 202106250912). All procedures were performed in accordance with the Guidance Suggestions for the Care and Use of Laboratory Animals, formulated by the Ministry of Science and Technology of China. All procedures performed in studies involving human participants were in accordance with the 1964 Helsinki declaration and its later amendments or comparable ethical standards. Written informed consent was obtained. We confirming the study is reported in accordance with ARRIVE guidelines.

Consent for publication
This manuscript does not contain personal and/or medical information about an identifiable living individual.

Competing interests
The authors declare no competing interests.

Received: 18 January 2024 / Accepted: 18 October 2024
Published online: 29 October 2024

References

1. Britt RD Jr., Ruwanpathirana A, Ford ML, Lewis BW. Macrophages Orchestrate Airway Inflammation, remodeling, and Resolution in Asthma. Int J Mol Sci 2023; 24.
2. Bantulà M, Arismendi E, Tubita V et al. Effect of obesity on the expression of genes Associated with severe Asthma-A pilot study. J Clin Med 2023; 12.
3. D'Avino D, Cerqua I, Ullah H et al. Beneficial effects of Astragalus membranaceus (Fisch.) Bunge Extract in Controlling Inflammatory Response and preventing asthma features. Int J Mol Sci 2023; 24.
4. Castillo JR, Peters SP, Busse WW. Asthma exacerbations: Pathogenesis, Prevention, and treatment. J Allergy Clin Immunol Pract. 2017;5:918–27.
5. Lv X, Dong M, Tang W, et al. Ferroptosis, novel therapeutics in asthma. Biomed Pharmacother. 2022;153:113516.
6. Wang X, Li Q, Sui B, Xu M, Pu Z, Qiu T. Schisandrin A from Schisandra chinensis Attenuates Ferroptosis and NLRP3 Inflammasome-Mediated Pyroptosis in Diabetic Nephropathy through Mitochondrial Damage by AdipoR1 Ubiquitination. Oxid Med Cell Longev 2022; 2022: 5411462.
7. Sarraf SA, Shah HV, Kanfer G, et al. Loss of TAX1BP1-Directed Autophagy results in protein aggregate Accumulation in the brain. Mol Cell. 2020;80:779–e795710.
8. Turco E, Savova A, Gere F, et al. Reconstitution defines the roles of p62, NBR1 and TAX1BP1 in ubiquitin condensate formation and autophagy initiation. Nat Commun. 2021;12:5212.
9. Fan Y, Cheng Z, Mao L, et al. PINK1/TAX1BP1-directed mitophagy attenuates vascular endothelial injury induced by copper oxide nanoparticles. J Nanobiotechnol. 2022;20:149.
10. Chua MD, Mineva GM, Guttman JA. Ube2N is present and functions within listeria actin-rich structures and lamellipodia: a localization and pharmacological inhibition study. Anat Rec (Hoboken). 2023;306:1140–8.
11. Li J, Qi C, Shao S, et al. SP1 transcriptionally regulates UBE2N expression to promote lung adenocarcinoma progression. Mol Biomed. 2023;4:7.
12. Chen YN, Shih CY, Guo SL, et al. Potential prognostic and predictive value of UBE2N, IMPDH1, DYNC1LI1 and HRASLS2 in colorectal cancer stool specimens. Biomed Rep. 2023;18:22.
13. Liu Y, Xu Y, Wang F, et al. Inhibition of AMPK activity by TRIM11 facilitates cell survival of hepatocellular carcinoma under metabolic stress. Clin Transl Med. 2021;11:e617.
14. Kuempers C, Jagomast T, Paulsen FO et al. TRIM11 expression in non-small cell lung cancer is associated with poor prognosis. Histol Histopathol 2023; 18647.
15. Pan Y, Yu H, Lu F. TRIM11 Posttranscriptionally modulated by miR-5193 facilitates tumor growth and metastasis of prostate Cancer. Technol Cancer Res Treat. 2023;22:15330338231178639.
16. Zhao Z, Deng J, Lu M, et al. TRIM11, a new target of p53, facilitates the migration and invasion of nasopharyngeal carcinoma cells. Mol Biol Rep. 2023;50:731–7.
17. Tan YY, Zhou HQ, Lin YJ, et al. FGF2 is overexpressed in asthma and promotes airway inflammation through the FGFR/MAPK/NF-κB pathway in airway epithelial cells. Mil Med Res. 2022;9:7.
18. Pu Z, Wang W, Xie H, Wang W. Apolipoprotein C3 (ApoC3) facilitates NLRP3 mediated pyroptosis of macrophages through mitochondrial damage by accelerating of the interaction between SCIMP and SYK pathway in acute lung injury. Int Immunopharmacol. 2024;128:111537.
19. Li L, Liu Z, Yang X, Yan H, Bao S, Fei J. Bioluminescence imaging for IL-1β expression in experimental colitis. J Inflamm (Lond). 2013;10:16.
20. Scioscia G, Tondo P, Nolasco S et al. Benralizumab in patients with severe eosinophilic asthma: a Multicentre Real-Life experience. J Clin Med 2023; 12.
21. Duh TH, Yang CJ, Lee CH, Ko YC. A study of the relationship between Phthalate exposure and the occurrence of adult asthma in Taiwan. Molecules 2023; 28.
22. Liu T, Tang Q, Liu K, et al. TRIM11 suppresses AIM2 inflammasome by degrading AIM2 via p62-Dependent selective autophagy. Cell Rep. 2016;16:1988–2002.
23. Li Y, Yan B, Wu Y, et al. Ferroptosis participates in dibutyl phthalate-aggravated allergic asthma in ovalbumin-sensitized mice. Ecotoxicol Environ Saf. 2023;256:114848.
24. Liu L, Zhou L, Wang LL, et al. Programmed cell death in Asthma: apoptosis, autophagy, Pyroptosis, ferroptosis, and Necroptosis. J Inflamm Res. 2023;16:2727–54.
25. Bao C, Liu C, Liu Q, et al. Liproxstatin-1 alleviates LPS/IL-13-induced bronchial epithelial cell injury and neutrophilic asthma in mice by inhibiting ferroptosis. Int Immunopharmacol. 2022;109:108770.
26. Shang M, Weng L, Xu G, et al. TRIM11 suppresses ferritinophagy and gemcitabine sensitivity through UBE2N/TAX1BP1 signaling in pancreatic ductal adenocarcinoma. J Cell Physiol. 2021;236:6868–83.
27. Verstrepen L, Verhelst K, Carpentier I, Beyaert R. TAX1BP1, a ubiquitin-binding adaptor protein in innate immunity and beyond. Trends Biochem Sci. 2011;36:347–54.
28. Waidmann O, Pleli T, Weigert A, et al. Tax1BP1 limits hepatic inflammation and reduces experimental hepatocarcinogenesis. Sci Rep. 2020;10:16264.

29. Cai M, Ding J, Li Y, et al. Echinococcus multilocularis infection induces UBE2N suppression via exosomal emu-miR-4989. Acta Trop. 2021;223:106087.
30. Barreyro L, Sampson AM, Ishikawa C, et al. Blocking UBE2N abrogates oncogenic immune signaling in acute myeloid leukemia. Sci Transl Med. 2022;14:eabb7695.
31. Shembade N, Ma A, Harhaj EW. Inhibition of NF-kappaB signaling by A20 through disruption of ubiquitin enzyme complexes. Science. 2010;327:1135–9.

Publisher's note